

Supporting Information

Atomically Dispersed Fe/Zn Synergy on Sulfur-Modified Nitrogen-Doped Carbon for Boosting Oxygen Reduction Activity

Ting Wang,^a Zongge Li,*^a Wenjun Kang,^a Rui Li,^a Konggang Qu,^a Lei Wang,^a Fanpeng Meng*^a and Haibo Li*^a

^a Shandong Provincial Key Laboratory of Chemical Energy Storage and Novel Cell Technology, School of Chemistry and Chemical Engineering, Liaocheng University, Liaocheng, Shandong, 252059 P. R. China.

*Correspondence authors. Email: lizongge@lcu.edu.cn; mengfanpeng@lcu.edu.cn; haiboli@mail.ustc.edu.cn.

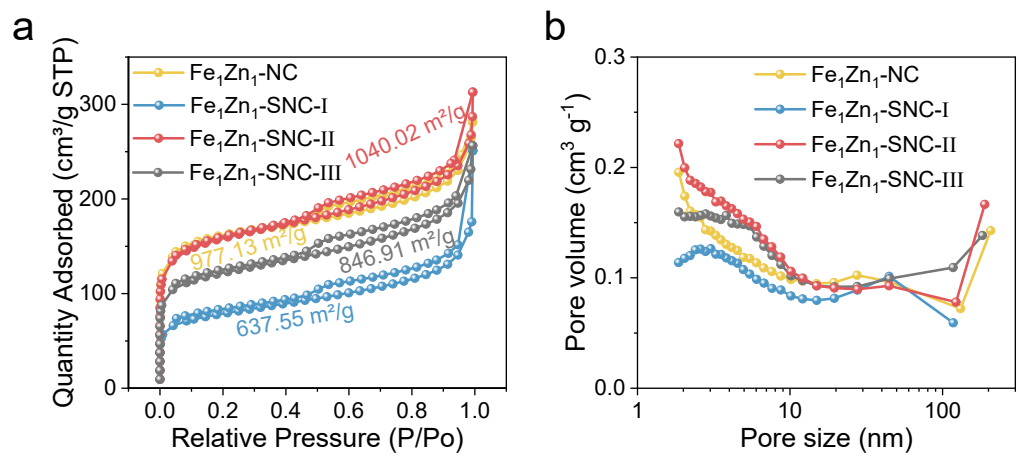


Fig. S1. (a) The surface area and (b) pore size of $\text{Fe}_1\text{Zn}_1\text{-NC}$, $\text{Fe}_1\text{Zn}_1\text{-SNC-I}$, $\text{Fe}_1\text{Zn}_1\text{-SNC-II}$ and $\text{Fe}_1\text{Zn}_1\text{-SNC-III}$.

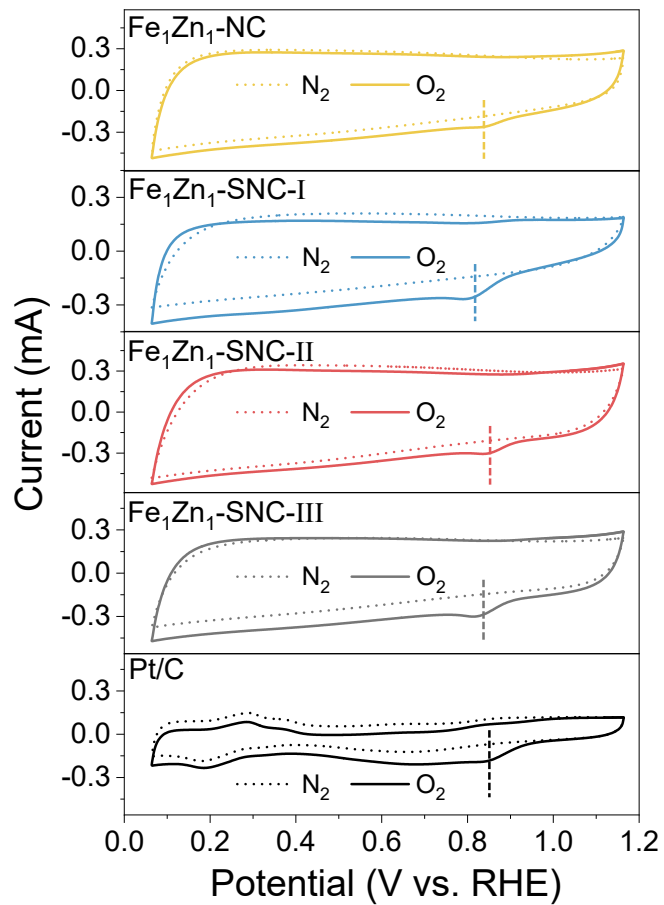


Fig. S2. CV curves in N_2 and O_2 of Fe₁Zn₁-NC, Fe₁Zn₁-SNC-X (X = I, II, III) and Pt/C.

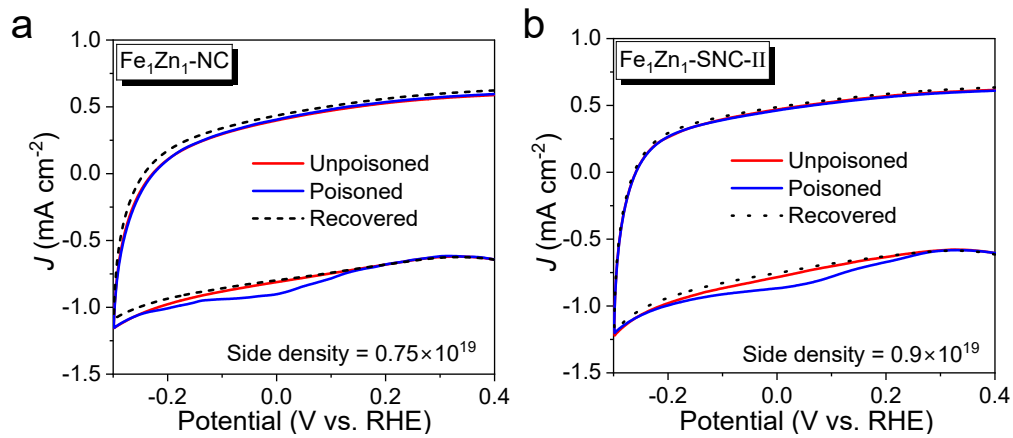


Fig. S3. Site density of (a) Fe₁Zn₁-NC and (b) Fe₁Zn₁-SNC-II through reversible nitrite poisoning in a 0.5 M acetate buffer at pH=5.4.

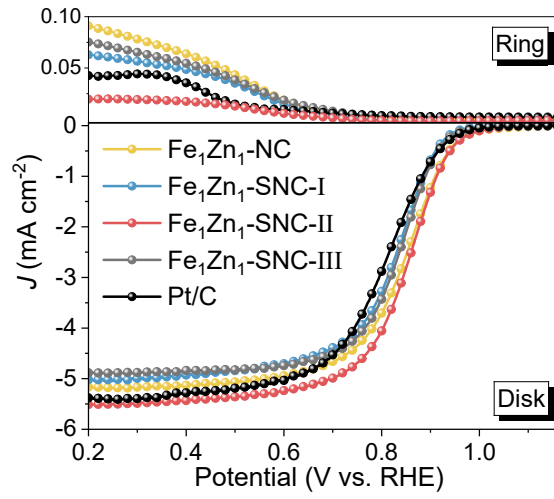


Fig. S4. LSV curves tested on the RRDE for all catalysts in an O_2 -saturated 0.1 M KOH at 1600 rpm.

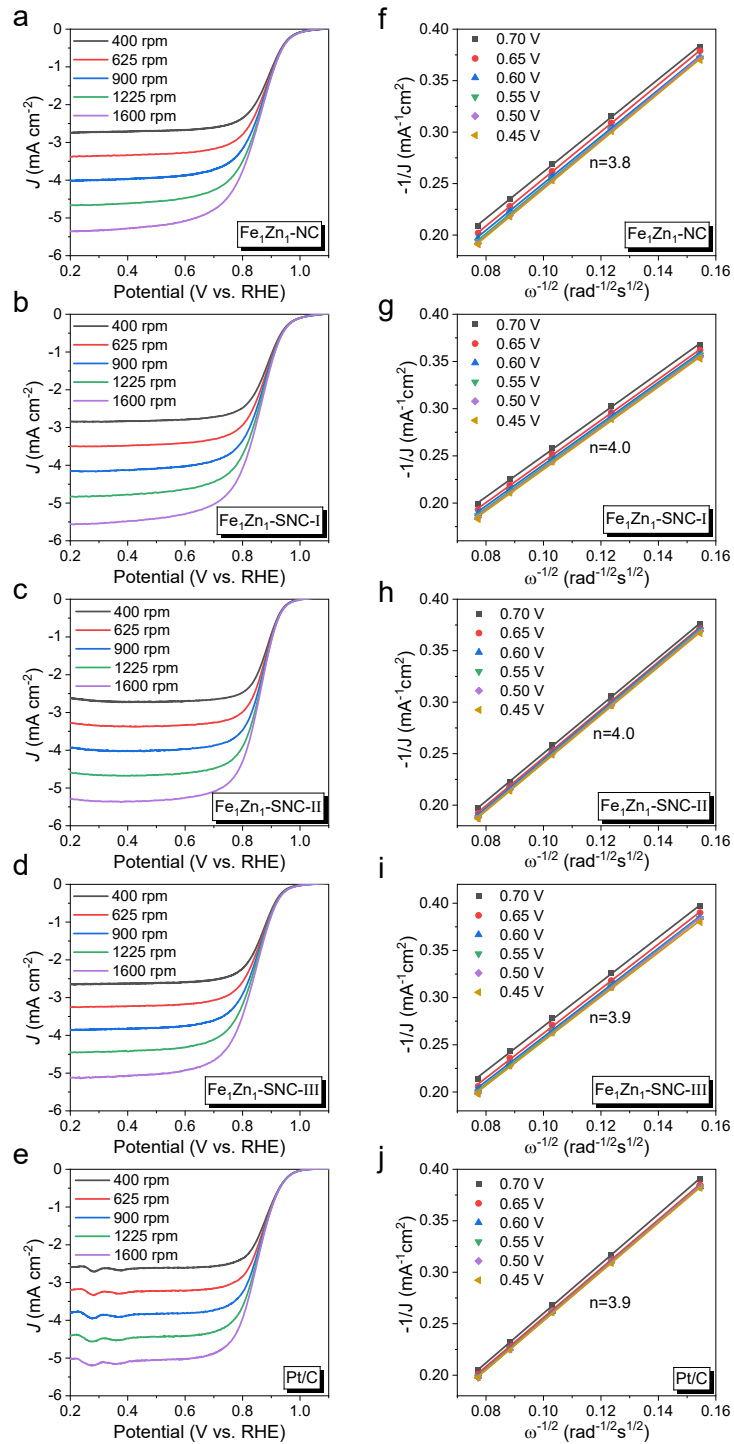


Fig. S5. LSV curves of (a) Fe₁Zn₁-NC, (b) Fe₁Zn₁-SNC-I, (c) Fe₁Zn₁-SNC-II, (d) Fe₁Zn₁-SNC-III and (e) Pt/C at different rotation speeds. Corresponding K-L plots of (g) Fe₁Zn₁-NC, (h) Fe₁Zn₁-SNC-I, (i) Fe₁Zn₁-SNC-II, (j) Fe₁Zn₁-SNC-III and (j) Pt/C.

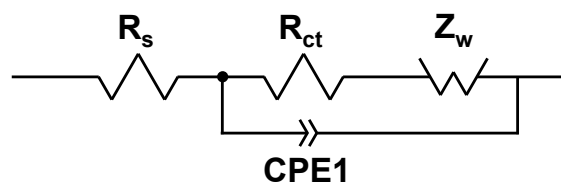


Fig. S6. Equivalent circuit corresponding to the EIS spectra.

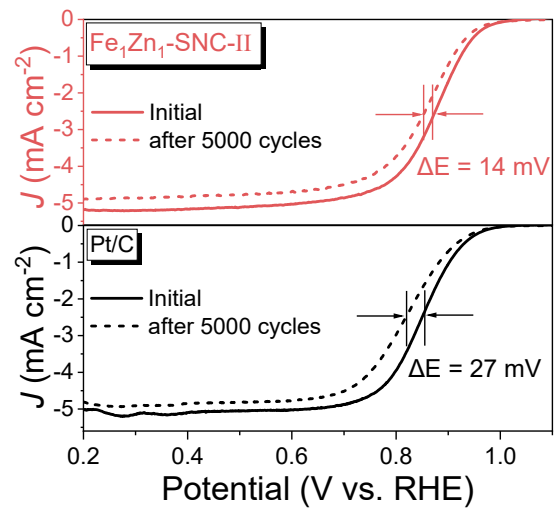


Fig. S7. Long-term cycling stability via an accelerated durability test (ADT).

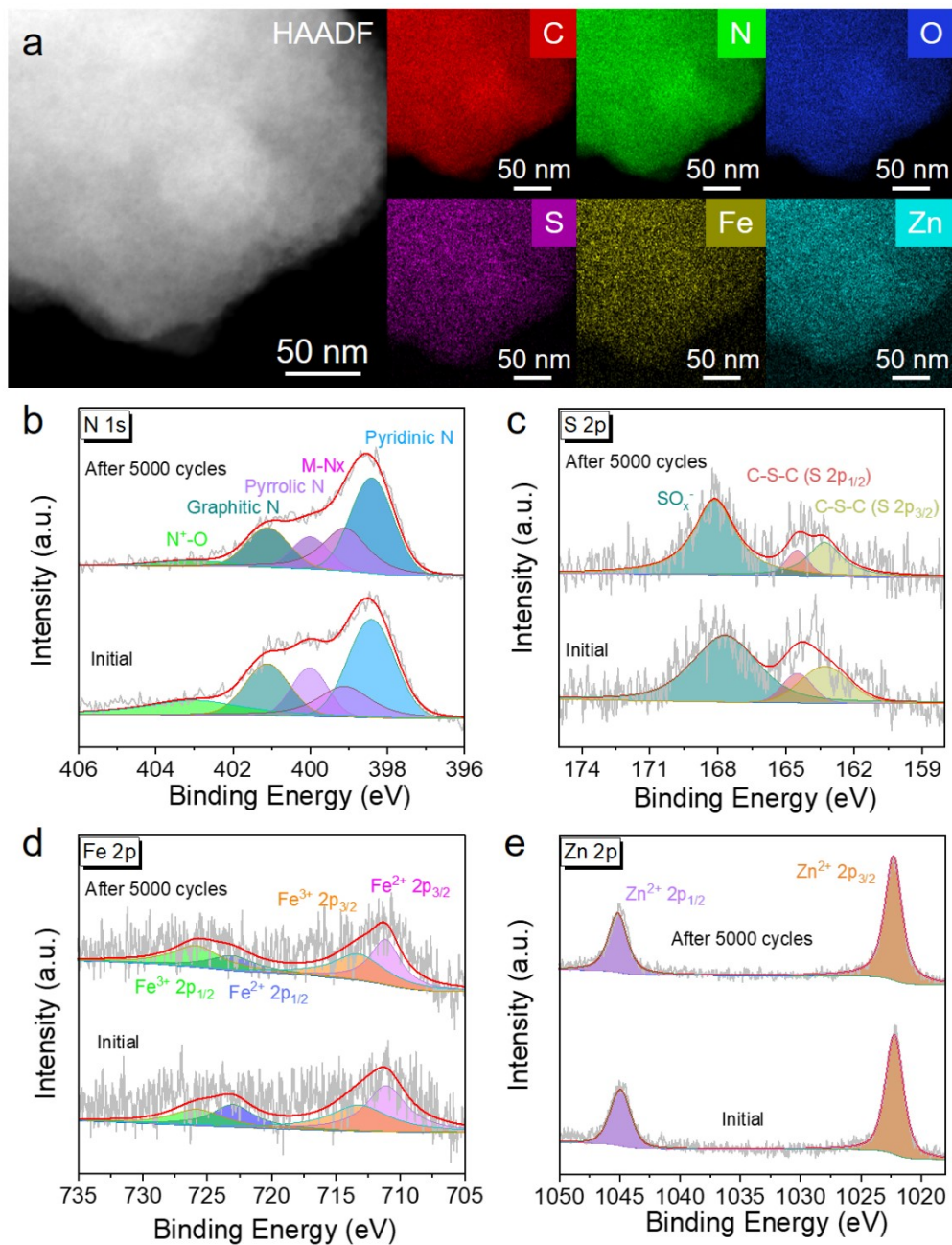


Fig. S8. (a) EDS mapping, (b) XPS N 1s spectra, (c) S 2p, (d) Fe 2p and (e) Fe 2p were examined after 5000 cycles of Fe₁Zn₁-SNC-II.

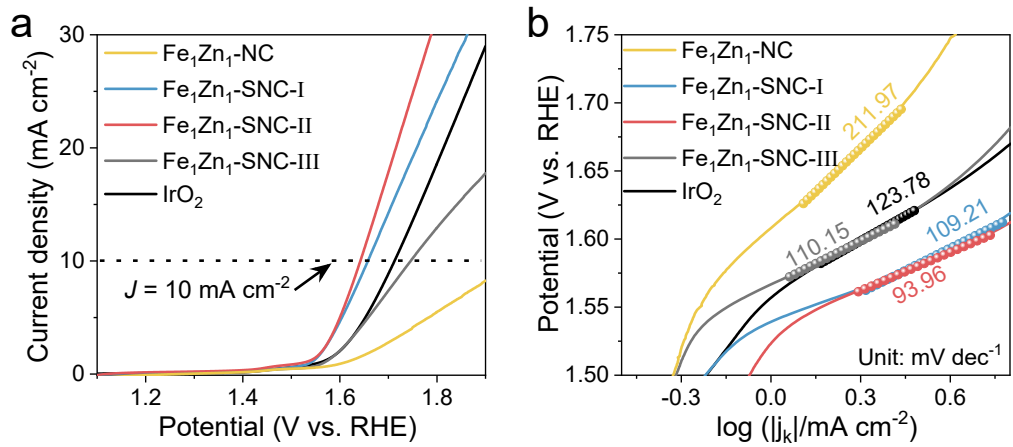


Fig. S9. (a) OER polarization curves and (b) Tafel plots of $\text{Fe}_1\text{Zn}_1\text{-NC}$, $\text{Fe}_1\text{Zn}_1\text{-SNC-I}$, $\text{Fe}_1\text{Zn}_1\text{-SNC-II}$, $\text{Fe}_1\text{Zn}_1\text{-SNC-III}$, and IrO_2 .

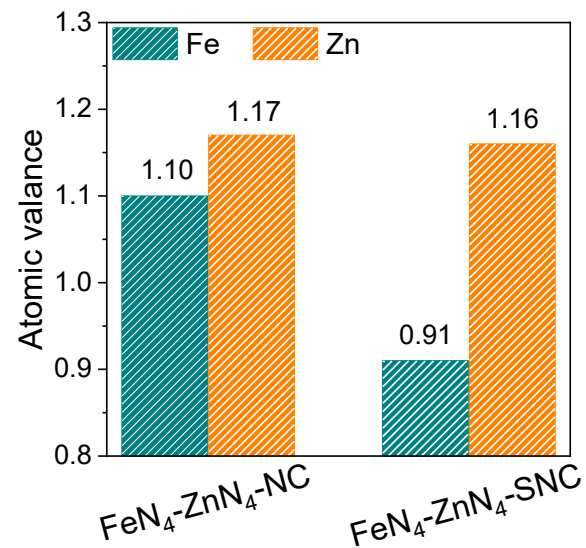


Fig. S10. Bader charge of Fe and Zn atoms in $\text{FeN}_4\text{-ZnN}_4\text{-NC}$ and $\text{FeN}_4\text{-ZnN}_4\text{-SNC}$.

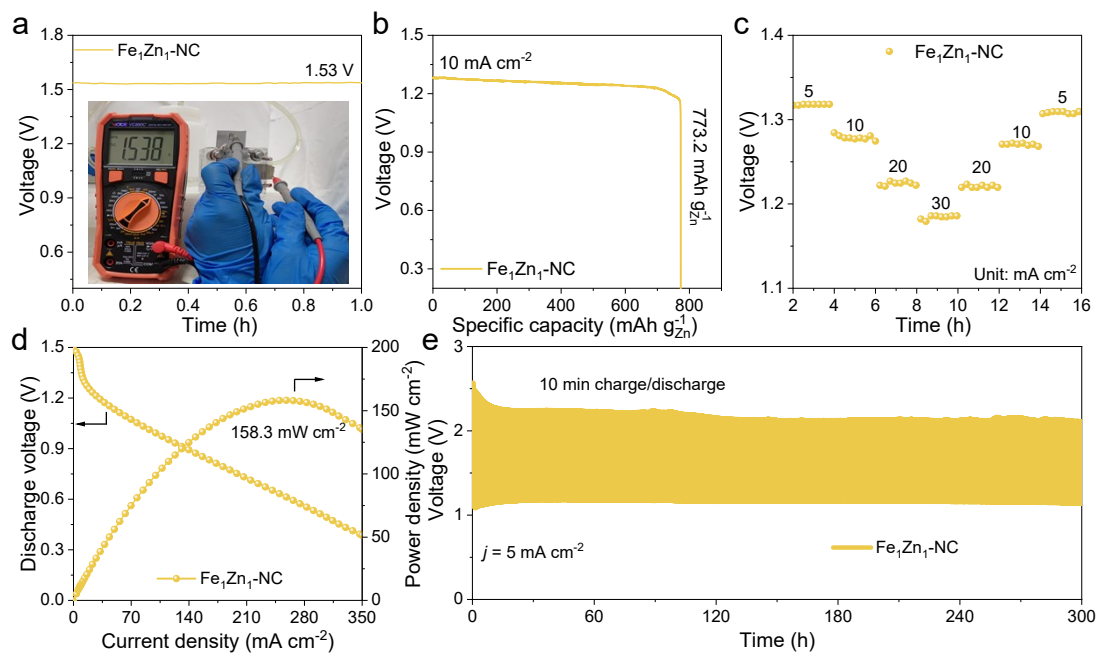


Fig. S11 (a) Open-circuit voltage plots, inset graphic shows voltage values. (b) Specific capacity curves at a current density of 10 mA cm^{-2} . (c) Galvanostatic discharge curves at various current densities. (d) Discharge polarization plots and power density curves and (e) charge–discharge cycling performance of the Zn-air battery assembled with $\text{Fe}_1\text{Zn}_1\text{-NC}$.

Table S1. Composition of various samples obtained using ICP analysis.

Catalysts	Elements	Fe (wt. %)	Zn (wt. %)
$\text{Fe}_1\text{Zn}_1\text{-NC}$		0.93	9.23
$\text{Fe}_1\text{Zn}_1\text{-SNC-}$ I		1.24	7.66
$\text{Fe}_1\text{Zn}_1\text{-SNC-}$ II		1.48	7.95
$\text{Fe}_1\text{Zn}_1\text{-SNC-}$ III		1.44	7.77

Table S2. EXAFS fitting parameters at the Fe K-edge for different structures.

	Shell	N^a	$R(\text{\AA})^b$	$\sigma^2(\text{\AA}^2)^c$	$\Delta E_0(\text{eV})^d$	R factor
Fe foil	Fe-Fe	8.0*	2.48 ± 0.02	0.0069	6.5 ± 2.6	0.0072
Fe_2O_3	Fe-O	5.9 ± 0.2	1.97 ± 0.03	0.0129		
	Fe-Fe	12.8 ± 0.7	3.09 ± 0.04	0.0354	4.9 ± 0.4	0.0089
FePc	Fe-N	4.2 ± 0.3	1.99 ± 0.02	0.0085	3.1 ± 0.7	0.0069
$\text{Fe}_1\text{Zn}_1\text{-SNC-II}$	Fe-N	4.1 ± 0.2	1.99 ± 0.03	0.0157	3.3 ± 0.2	0.0125

^a N : coordination numbers; ^b R : bond distance; ^c σ^2 : Debye-Waller factors; ^d ΔE_0 : the inner potential correction. R factor: goodness of fit. S_0^2 was set to 1.063, according to the experimental EXAFS fit of metal foil reference by fixing N as the known crystallographic value.

Table S3. EXAFS fitting parameters at the Zn K-edge for different structures.

	Shell	N^a	$R(\text{\AA})^b$	$\sigma^2(\text{\AA}^2)^c$	$\Delta E_0(\text{eV})^d$	R factor
Zn foil	Zn-Zn	6*	2.64 ± 0.02	0.0124	2.7 ± 1.3	0.0146
ZnO	Zn-O	6.2 ± 0.3	1.95 ± 0.02	0.0034		
	Zn-Zn	12.4 ± 0.2	3.25 ± 0.03	0.0181	3.5 ± 0.9	0.0225
ZnPc	Zn-N	4.1 ± 0.1	1.99 ± 0.01	0.0056	6.9 ± 0.5	0.0167
Fe ₁ Zn ₁ -SNC-II	Zn-N	3.8 ± 0.3	2.01 ± 0.02	0.0067	7.9 ± 1.6	0.0157

^a N : coordination numbers; ^b R : bond distance; ^c σ^2 : Debye-Waller factors; ^d ΔE_0 : the inner potential correction. R factor: goodness of fit. S_0^2 was set to 1.050, according to the experimental EXAFS fit of metal foil reference by fixing N as the known crystallographic value.

Table S4. Site density of Fe₁Zn₁-NC and Fe₁Zn₁-SNC-II.

Sample	Site density (mol g ⁻¹) ¹⁾	Site density (μmol g ⁻¹) ¹⁾
Fe ₁ Zn ₁ -NC	0.75×10 ¹⁹	12.4
Fe ₁ Zn ₁ -SNC-II	0.9×10 ¹⁹	14.9

Table S5. The simulated equivalent circuit data of the catalysts.

Catalysts	R _s ($\Omega \text{ cm}^{-2}$)	R _{ct} ($\Omega \text{ cm}^{-2}$)	CPE-T	CPE-P
Fe ₁ Zn ₁ -NC	7.098	59.72	5.29E-9	0.990
Fe ₁ Zn ₁ -SNC-I	12.12	60.87	2.95E-9	1.019
Fe ₁ Zn ₁ -SNC-II	7.277	53.52	4.44E-9	0.970
Fe ₁ Zn ₁ -SNC-III	9.623	59.54	2.39E-9	1.010

Table S6. Performance comparison of non-noble metal catalysts reported in recent literature

Catalysts	$E_{1/2}$ (V)	OCV (V)	Power density (mW cm ⁻²)	Specific capacity (mAh g ⁻¹ _{Zn})	Tafel plots (mV dec ⁻¹)
This work	0.871	1.58	228	804	78.69
Pt/C in this work	0.849	1.49	185	762	91.95
NPS-HPCNF ^[1]	0.86	1.51	210	795	67.4
Zn/Fe-NC ^[2]	0.875	1.46	186	815	-
A-MnO ₂ /NSPC-2 ^[3]	0.87	1.54	181	816	91
Fe/Cu-N-C ^[4]	0.89	1.50	116.6	809.2	69.4
FeCu SACs/NC ^[5]	0.89	1.48	153	741.0	68.6
Fe–N,O/G ^[6]	0.86	1.55	164.7	-	90
Co ₃ S ₄ /FeS@CoFe/NC ^[7]	0.872	1.34	170	816.3	45
Fe SAs/NG ^[8]	0.883	1.51	272.6	798	91.7
Fe@NC-2-900 ^[9]	0.86	1.50	198	867	90.1
Co ₃ O _{4-x} @N-C-2 ^[10]	0.845	1.524	105.2	799.5	73.1

1. X. Xu, H. Wu, Y. Yan, Y. Zheng, Y. Yan, S. Qiu, T. Liang, C. Deng, Y. Yao, J. Zou and M. Liu, *Adv. Energy Mater.*, 2025, **15**, 2405236.
2. C. Fu, X. Qi, L. Zhao, T. Yang, Q. Xue, Z. Zhu, P. Xiong, J. Jiang, X. An, H. Chen, J. S. Chen, A. Cabot and R. Wu, *Appl. Catal., B*, 2023, **335**, 122875.
3. L. Huo, M. Lv, M. Li, X. Ni, J. Guan, J. Liu, S. Mei, Y. Yang, M. Zhu, Q. Feng, P. Geng, J. Hou, N. Huang, W. Liu, X. Y. Kong, Y. Zheng and L. Ye, *Adv. Mater.*, 2024, **36**, 2312868.
4. W. Zhang, B. Feng, L. Huang, Y. Liang, J. Chen, X. Li, Z. Shi and N. Wang, *Appl. Catal., B*, 2024, **358**, 124450.
5. H. Liu, L. Jiang, Y. Wang, X. Wang, J. Khan, Y. Zhu, J. Xiao, L. Li and L. Han, *Chem. Eng. J.*, 2023, **452**, 138938.
6. Y. Li, Y. Ding, B. Zhang, Y. Huang, H. Qi, P. Das, L. Zhang, X. Wang, Z.-S. Wu and X. Bao, *Energy Environ. Sci.*, 2023, **16**, 2629-2636.
7. Y. Tan, Y. Wang, A. Li, X. Jiang, Y. Zhang and C. Cheng, *J. Energy Chem.*, 2024, **96**, 568-577.

8. Y. Deng, Y. Lin, M. Zhang, Y. Lu, W. Zhang, W. Zhang, Z. Zhang, M. Xiang, H. Gu and J. Bai, *Int. J. Hydrogen Energy*, 2024, **65**, 905-911.
9. Z. Luo, L. He, J. Wu, Y. Tian, M. Yang, X. Liu, R. Zheng and D. Zhang, *ChemSusChem*, 2025, **18**, e202401552.
10. Y. Wang, R. Gan, Z. Ai, H. Liu, C. Wei, Y. Song, M. Dirican, X. Zhang, C. Ma and J. Shi, *Carbon*, 2021, **181**, 87-98.